

Spectral rigidity of vehicular streams (random matrix theory approach)

Milan Krbálek^{1,2} and Petr Šeba^{2,3,4}

¹ Faculty of Nuclear Sciences and Physical Engineering, Czech Technical University, Prague, Czech Republic

² Doppler Institute for Mathematical Physics and Applied Mathematics, Faculty of Nuclear Sciences and Physical Engineering, Czech Technical University, Prague, Czech Republic

³ University of Hradec Králové, Hradec Králové, Czech Republic

⁴ Institute of Physics, Academy of Sciences of the Czech Republic, Prague, Czech Republic

Received 16 April 2009, in final form 24 June 2009

Published 31 July 2009

Online at stacks.iop.org/JPhysA/42/345001

Abstract

Using a method originally developed for the random matrix theory, we derive an approximate mathematical formula for the number variance $\Delta_N(L)$ describing the rigidity of particle ensembles with a power-law repulsion. The resulting relation is compared with the relevant statistics of the single-vehicle data measured on the Dutch freeway A9. The detected value of the inverse temperature β , which can be identified as a coefficient of the mental strain of the car drivers, is then discussed in detail with the relation to the traffic density ρ and flow J .

PACS numbers: 05.40.-a, 89.40.-a, 05.45.-a

(Some figures in this article are in colour only in the electronic version)

1. Terminus a quo

The main goal of this paper is to show that the statistical fluctuations of the single-vehicle data (in vehicular flows) can very well be predicted by the methods known from the random matrix theory. Beyond that, we intend to demonstrate that the changes of the statistical variances in the vehicular samples depend not only on the macroscopical traffic quantities and the three traffic phases (the free flow, synchronized flow and the wide moving jams as published in [1] or [2]), but also on the psychological characteristics of the driver's decision-making process. We will illustrate that the transitions among the three traffic phases cause perceptible changes in the mental strain of the car drivers.

As reported in [1–5], the three traffic phases show substantially different microscopical properties. It was demonstrated in [6–9] that the microscopical traffic structure can be estimated with the help of a repulsive potential (applied locally only) describing the mutual

interaction between the successive cars in the chain of vehicles. Especially, the probability density $\wp(r)$ for the distance r between two successive cars (*clearance distribution*) can be derived by the means of a one-dimensional gas with an inverse temperature β and interacting by the repulsive potential $V(r) = r^{-1}$ (as discussed in [6–8]). In particular, denoting Heaviside’s function by $\Theta(x)$

$$\Theta(x) = \begin{cases} 1, & x > 0 \\ 0, & x \leq 0, \end{cases}$$

and the modified Bessel’s function of the second kind (Macdonald’s function) by $\mathcal{K}_\lambda(x)$, the clearance distribution of the above-mentioned thermodynamical traffic gas reads

$$\wp(r) = \mathcal{A}\Theta(r) e^{-\beta/r} e^{-Br}, \tag{1}$$

where

$$B = \beta + \frac{3 - e^{-\sqrt{\beta}}}{2}, \tag{2}$$

$$\mathcal{A}^{-1} = 2\sqrt{\frac{\beta}{B}}\mathcal{K}_1(2\sqrt{B\beta}). \tag{3}$$

We remark that $\wp(r)$ fulfills two normalization conditions

$$\int_{\mathbb{R}} \wp(r) dr = 1 \tag{4}$$

and

$$\int_{\mathbb{R}} r \wp(r) dr = 1. \tag{5}$$

The latter represents a scaling to a mean clearance equal to 1. Distribution (1) is in good agreement with the clearance distribution observed with the real-road data ([4, 6–8]). The inverse temperature β of the gas is related to the traffic density ρ . We note that β can be understood as a quantitative description of the mental strain of the drivers in a given traffic situation. More specifically, the parameter β reflects the psychological pressure under which the driver stays while moving in the traffic stream. Whereas the free flows induce practically no mental strain of the drivers, with the increasing traffic density the mental strain escalates rapidly. This will be confirmed in the following sections.

2. Statistical variances in traffic data

Another powerful way to inspect the interactions between the cars within the highway data is to investigate the traffic flow fluctuations. One possibility is to use the so-called *time-gap variance* Δ_T considered in the paper [10] and defined as follows. Let $\{t_i : i = 1, \dots, Q\}$ be a data set of the time intervals between two subsequent cars passing a fixed point on the highway. Using it one can calculate the moving average

$$T_k^{(N)} = \frac{1}{N} \sum_{i=k}^{k+N-1} t_i \quad (k = 1, \dots, Q - N + 1)$$

of the time intervals produced by the $N + 1$ successive vehicles (i.e. N gaps) as well as the total average

$$\bar{T} = \frac{1}{Q} \sum_{i=1}^Q t_i \equiv T_1^{(Q)}.$$

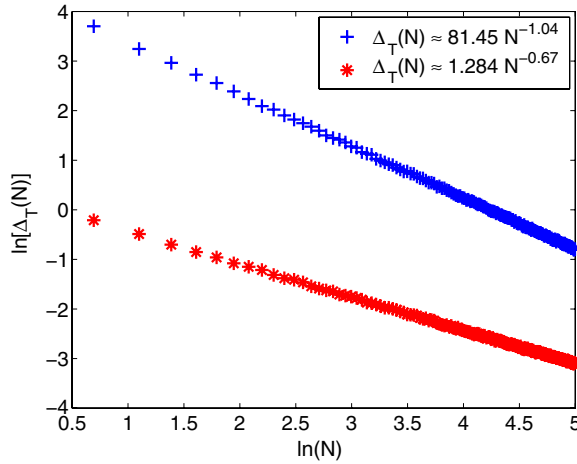


Figure 1. The time-gap variance $\Delta_T(N)$ as a function of the sampling size N (on a log–log scale). Plus signs and stars represent the variance of the average time-gaps for the free and congested flows, respectively.

The time-gap variance Δ_T is defined by the variance of the sample-averaged time intervals as a function of the sampling size N ,

$$\Delta_T = \frac{1}{Q - N + 1} \sum_{k=1}^{Q-N+1} (T_k^{(N)} - \bar{T})^2,$$

where k runs over all possible samples of $N + 1$ successive cars. For time intervals t_i being statistically independent, the law of large numbers gives $\Delta_T(N) \propto 1/N$.

The statistical analysis of a data set recorded on the Dutch freeway A9 and published in [10] leads, however, to different results—see figure 1. For the free traffic flow ($\rho < 15 \text{ veh km}^{-1} \text{ lane}^{-1}$) one observes indeed the expected behavior $\Delta_T(N) \propto 1/N$. More interesting behavior, nevertheless, is detected for higher densities ($\rho > 35 \text{ veh km}^{-1} \text{ lane}^{-1}$). In this case, a power-law dependence was found by Nishinari *et al* [10]:

$$\Delta_T(N) \propto N^\epsilon$$

with the exponent $\epsilon \approx -2/3$. So the intervals are not independent, and the exponent ϵ reflects the correlations between the vehicles in a congested traffic flow.

There is, however, one substantial drawback of this description. The time-gap variance was introduced *ad hoc*, and hardly anything is known about its exact mathematical properties in the case of interacting vehicles. It is, therefore, appropriate to look for an alternative description that is mathematically well understood. A natural candidate is the *number variance* $\Delta_N(L)$ that was originally introduced for describing a *spectral rigidity* of the eigenvalues in random matrix theory. $\Delta_N(L)$ also gives the variances in the particle positions of a certain class of one-dimensional interacting gases (for example, a Dyson gas in [12]) and it is defined as follows: consider a set $\{r_i : i = 1, \dots, Q\}$ of distances (i.e. *clearances* in the traffic terminology) between each pair of subsequent cars moving in the same lane. We suppose that the mean distance taken over the complete set is re-scaled to 1, i.e.

$$\sum_{i=1}^Q r_i = Q.$$

Dividing the interval $[0, Q]$ into subintervals $[(k - 1)L, kL]$ of a length L and denoting by $n_k(L)$ the number of cars in the k th subinterval, the average value $\bar{n}(L)$ taken over all possible subintervals is

$$\bar{n}(L) = \frac{1}{\lfloor Q/L \rfloor} \sum_{k=1}^{\lfloor Q/L \rfloor} n_k(L) = L,$$

where the integer part $\lfloor Q/L \rfloor$ stands for the number of all subintervals $[(k - 1)L, kL]$ included in the interval $[0, Q]$. We suppose, for convenience, that Q/L is an integer, i.e. $\lfloor Q/L \rfloor = Q/L$. The number variance $\Delta_N(L)$ is then defined as

$$\Delta_N(L) = \frac{L}{Q} \sum_{k=1}^{Q/L} (n_k(L) - L)^2$$

and represents the statistical variance of the number of vehicles moving at the same time inside a fixed part of the road of a length L . The mathematical properties of the number variance are well understood. So $\Delta_N(L)$ serves as a better alternative for the description of the traffic fluctuations (a rigidity of the vehicular chain) than the time-gap variance $\Delta_T(N)$ itself (see also [4]).

3. The exact formula for number variance

Knowing the one-parameter family of the probability densities (1), we can derive an approximate formula for the rigidity $\Delta_N(L)$ of the related thermodynamical traffic gas (see [7]). We use a method presented in [11, 12] in detail.

Let $\wp_n(r)$ represent the n th nearest-neighbor probability density (n th probability density for short), i.e. the probability density for the spacing r between the $n + 2$ neighboring particles. The probability density for the spacing between two succeeding particles (cars) is $\wp(r) = \wp_0(r)$. Regarding the spacings as independent, the n th probability density $\wp_n(r)$ can be calculated via the recurrent formula

$$\wp_n(r) = \wp_{n-1}(r) \star \wp_0(r),$$

where the symbol \star represents a convolution of the two probabilities, i.e.

$$\wp_n(r) = \int_{\mathbb{R}} \wp_{n-1}(s) \wp_0(r - s) ds.$$

Using the method of mathematical induction and an approximation of the function

$$g_n(r, s) = e^{-\beta\left(\frac{n^2}{s} + \frac{1}{r-s}\right)} \approx e^{-\frac{\beta}{r}(n+1)^2}$$

in the saddle point, one can obtain

$$\begin{aligned} \wp_n(r) &= \Theta(r) \int_0^r \mathcal{N}_{n-1} \mathcal{N}_0 s^{n-1} e^{-\beta\frac{n^2}{s}} e^{-Bs} e^{-\frac{\beta}{r-s}} e^{-B(r-s)} ds \\ &= \Theta(r) \mathcal{N}_{n-1} \mathcal{N}_0 e^{-Br} \int_0^r s^{n-1} g_n(r, s) ds \\ &\approx \Theta(r) \mathcal{N}_{n-1} \mathcal{N}_0 e^{-\frac{\beta}{r}(n+1)^2} e^{-Br} \int_0^r s^{n-1} ds \\ &\approx \Theta(r) \mathcal{N}_{n-1} \mathcal{N}_0 n^{-1} r^n e^{-\frac{\beta}{r}(n+1)^2} e^{-Br}. \end{aligned}$$

Hence

$$\wp_n(r) \approx \Theta(r) \mathcal{N}_n r^n e^{-\frac{\beta}{r}(n+1)^2} e^{-Br},$$

where (after applying the re-normalization procedure)

$$\mathcal{N}_n^{-1} = 2 \left(\sqrt{\frac{\beta}{B}} (n+1) \right)^{n+1} \mathcal{K}_{n+1}(2(n+1)\sqrt{B\beta}).$$

This fixes the proper normalization $\int_{\mathbb{R}} \wp_n(r) dr = 1$. In addition to this the mean spacing equals

$$\int_{\mathbb{R}} r \wp_n(r) dr = n + 1.$$

According to [12] the variance $\Delta_N(L)$ can be evaluated by the formula

$$\Delta_N(L) = L - 2 \int_0^L (L-r)(1-R(r)) dr, \tag{6}$$

where

$$R(r) = \sum_{n=0}^{\infty} \wp_n(r)$$

is the *two-point cluster function*. A convenient way to calculate the asymptotic behavior of the variance $\Delta_N(L)$ for large L is the application of the Laplace transformation to the two-point cluster function $y(t) = \int_{\mathbb{R}} R(r) e^{-rt} dr$. It leads to a partial result:

$$y(t) = \sum_{n=0}^{\infty} \left(\frac{B}{B+t} \right)^{\frac{n+1}{2}} \frac{\mathcal{K}_{n+1}(2(n+1)\sqrt{(B+t)\beta})}{\mathcal{K}_{n+1}(2(n+1)\sqrt{B\beta})}.$$

The asymptotic behavior of Macdonald's function

$$\mathcal{K}_n(x) \approx \frac{2^{n-1} \Gamma(n)}{x^n} e^{-x} \quad (x \ll 1),$$

(where $\Gamma(x)$ represents the gamma function) provides the approximation

$$y(t) \approx \left(\frac{B+t}{B} \frac{e^{2\sqrt{(B+t)\beta}}}{e^{2\sqrt{B\beta}}} - 1 \right)^{-1}.$$

Applying Maclaurin's expansion (Taylor's expansion about the point zero) to the function $h(t) = t \cdot y(t)$ of order t^2 we obtain

$$y(t) \approx \frac{1}{t} + \alpha_0 + \alpha_1 t + \mathcal{O}(t^2),$$

where

$$\alpha_0 = -\frac{2B\beta + 3\sqrt{B\beta}}{4(1 + \sqrt{B\beta})^2},$$

$$\alpha_1 = \frac{6\sqrt{B\beta} + B\beta(21 + 4B\beta + 16\sqrt{B\beta})}{48B(1 + 2\sqrt{B\beta})^3}.$$

With the help of equation (6) and the inverse Laplace transform

$$R(r) = \frac{1}{2\pi i} \lim_{\varphi \rightarrow \infty} \int_{c-i\varphi}^{c+i\varphi} y(t) e^{rt} dt,$$

we finally get

$$\Delta_N(L) = \chi L + \gamma + \mathcal{O}(L^{-1}), \tag{7}$$

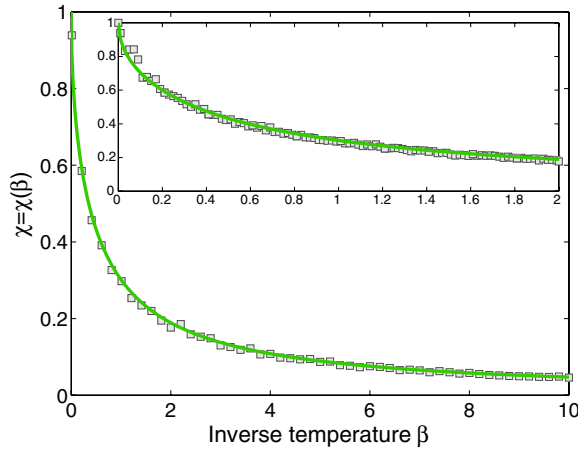


Figure 2. The slope $\chi(\beta)$ of the number variance $\Delta_N(L) \approx \chi L + \gamma$ as a function of the inverse temperature β . The squares represent the result of numerical calculations, whereas the continuous curve displays result (8) obtained mathematically. The behavior close to the origin is magnified in the inset.

where

$$\chi = \chi(\beta) = \frac{2 + \sqrt{B\beta}}{2B(1 + \sqrt{B\beta})} \quad (8)$$

and

$$\gamma = \gamma(\beta) = \frac{6\sqrt{B\beta} + B\beta(21 + 4B\beta + 16\sqrt{B\beta})}{24(1 + \sqrt{B\beta})^4}. \quad (9)$$

So the number variance displays a linear dependence (7) for large L . The correctness of the approximation is demonstrated in figures 2 and 3 where we have compared this result with the numerical simulation.

4. The number variance of the traffic data

As already discussed, the behavior of the number variance is sensitive to the temperature β —in the terminology of the Random Matrix Theory—or to the universality class of the random matrix ensemble. To use the known mathematical results, one need not mix together states with different densities—a procedure known as *data unfolding* in the Random Matrix Theory. For transportation, this means that one cannot mix together traffic states with different traffic densities (as published in [10]) and hence with a different vigilance of drivers. So we will perform a separate analysis of the data samples lying within short density intervals to prevent the undesirable mixing of different states.

We divide the region of the measured densities $\rho \in [0, 85 \text{ veh km}^{-1} \text{ lane}^{-1}]$ into 85 equidistant subintervals and analyze the data from each of them separately. The number variance $\Delta_N(L)$ evaluated with the data in a fixed density interval has a characteristic linear tail (see figure 4) that is well known from the Random Matrix Theory. Similarly, such a behavior was found in models of one-dimensional thermodynamical gases with the nearest-neighbor repulsion among the particles (see [11]). We recall that when the interaction is not restricted to the nearest neighbors but includes all particles, the number variance has typically

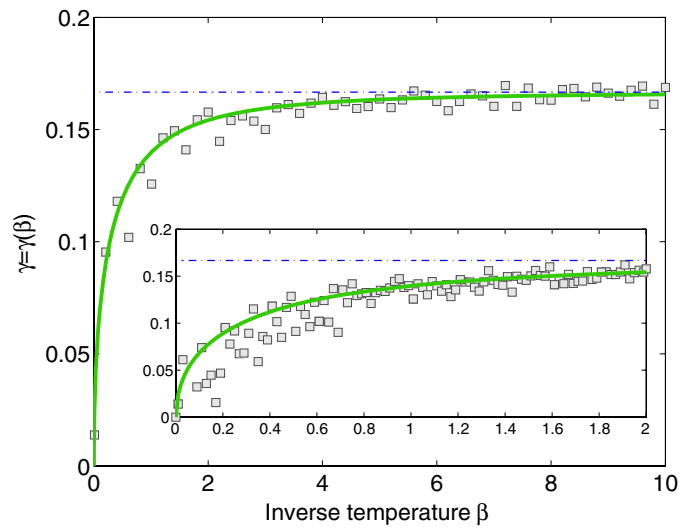


Figure 3. The shift $\gamma(\beta)$ of the number variance $\Delta_N(L) \approx \chi L + \gamma$ as a function of the inverse temperature β . The squares represent the results of numerical calculations whereas the curve shows the result (9). The behavior close to the origin is magnified in the inset. The dash-dotted line displays the asymptotic tendency in $\gamma = \gamma(\beta)$, i.e. $\lim_{\beta \rightarrow \infty} \gamma(\beta) = 1/6$.

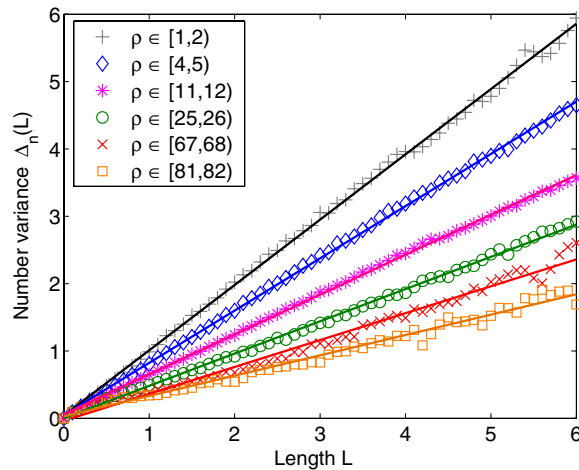


Figure 4. The number variance $\Delta_N(L)$ as a function of the length L . Plus signs, diamonds, stars, circles, crosses and squares represent the number variances of the real-road data in the given density regions (see the legend for details). The curves show the linear approximations of the individual data. Their slopes were analyzed and visualized in figure 5 (top part).

a logarithmical tail—see [12]. So the linear tail of $\Delta_N(L)$ supports the view that the traffic stream interactions are indeed restricted to the few nearest cars only. The slope of the linear tail of $\Delta_N(L)$ decreases with the traffic density (see the top subplot in figure 5). It is a consequence of the increasing alertness of the drivers and hence of the increasing coupling between the neighboring cars in the dense traffic flows.

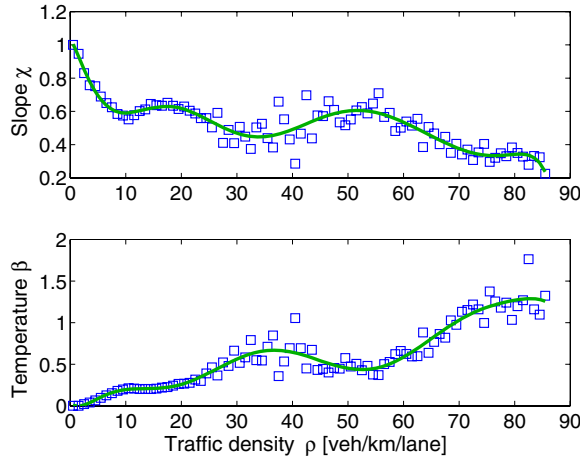


Figure 5. The slope χ and the inverse temperature β as functions of the traffic density ρ . The squares in the upper subplot display the slope of the number variance $\Delta_N(L)$ (see figure 4), separately evaluated for the various traffic densities. The lower subplot visualizes the corresponding values of the inverse temperature β . The continuous curves represent a polynomial approximations of the relevant data.

The theoretical properties of the function $\Delta_N(L)$ agree with the behavior of the number variance evaluated from the traffic data (see figure 4). The comparison with formula (7) allows us to determine the empirical dependence of the inverse temperature β on the traffic density ρ . The inverse temperature reflects the microscopic status of the individual vehicular interaction. Conversely, in the macroscopic approach, the traffic is treated as a continuum and modeled by aggregated fluid-like quantities, such as the density and the traffic flow (see [1, 2]). Its most prominent result is the dependence of the traffic flow on the traffic density—the fundamental diagram.

It is clear that the macroscopic traffic characteristics are determined by their microscopic status. Consequently, there should be a relation between the behavior of the fundamental diagram and that of the inverse temperature β . In figure 6, we display the behavior of the inverse temperature β simultaneously with the fundamental diagram. Both curves show a virtually linear increase in the region of the free traffic (up to $\rho \approx 10$ veh km⁻¹ lane⁻¹). The inverse temperature β then displays a plateau for the densities up to 18 veh km⁻¹ lane⁻¹ while the flow continues to increase. A detailed inspection uncovers, however, that the increase of the traffic flow ceases to be linear and becomes concave at that region. So the flow is reduced with respect to the outcome expected for a linear behavior—a manifestation of the onset of the phenomenon that finally leads to a congested traffic. For larger densities the temperature β increases up to $\rho \approx 32$ veh km⁻¹ lane⁻¹. The center of this interval is localized at $\rho \approx 25$ —a critical point of the fundamental diagram at which the flow starts to decrease. This behavior of the inverse temperature is understandable and imposed by the fact that the drivers, moving quite fast in a relatively dense traffic flow, have to synchronize their driving with the preceding car (a strong interaction) and are therefore under a considerable psychological pressure. After the transition from the free to the congested traffic regime (between 40 and 50 veh km⁻¹ lane⁻¹), the synchronization continues to decline because of the decrease of the mean velocity leading to decreasing β . Finally—for densities related to the congested traffic—the inverse temperature increases while the flow remains constant. The comparison between the traffic flow and the inverse temperature is even more illustrative when

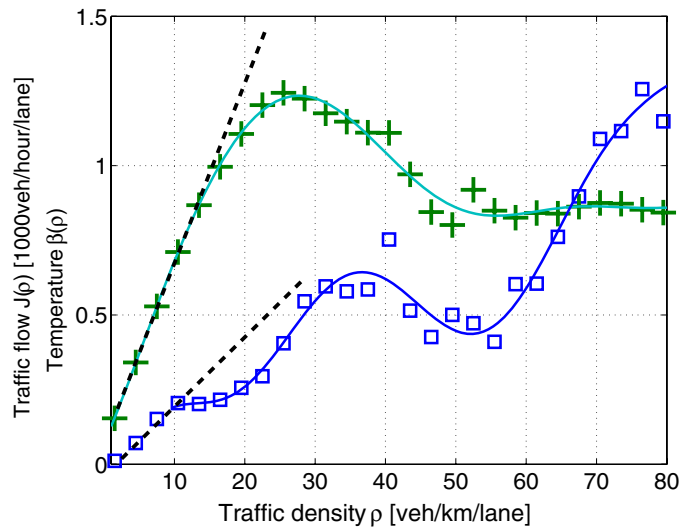


Figure 6. The traffic flow $J(\rho)$ and the inverse temperature $\beta(\rho)$ as functions of the traffic density ρ . Plus signs display the traffic flow in thousands of vehicles per hour and the squares correspond to the inverse temperature of the traffic gas. The results of a polynomial curve fitting are visualized by continuous curves. Dashed lines represent a linear approximations of the relevant data near the origin.

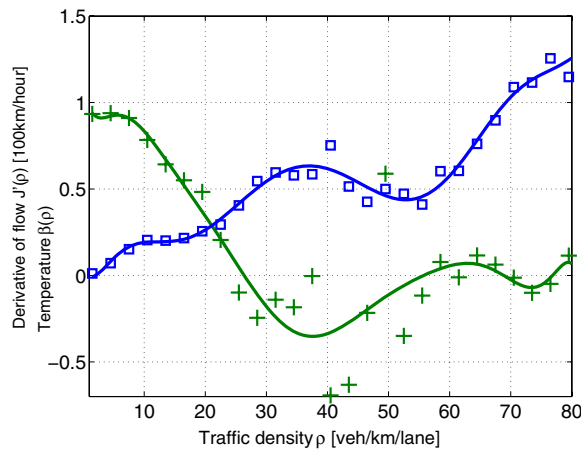


Figure 7. The inverse temperature $\beta(\rho)$ and the first derivative $J' = J'(\rho)$ as functions of the traffic density ρ . The squares correspond to the inverse temperature of the traffic sample while the plus signs display the average value of $J' = J'(\rho)$ (in kilometers per hour). The continuous curves represent a relevant polynomial approximations.

the changes of the flow are taken into account. Therefore, we evaluate the derivative of the flow

$$J' = \frac{\partial J}{\partial \rho}.$$

The result of the evaluation can be seen in figure 7 where one can trace the significant similarity between the shape of $J' = J'(\rho)$ and inverse temperature β .

5. Summary and conclusion

Using the methods developed by the Random Matrix Theory we have obtained an approximate formula for the number variance $\Delta_N(L)$ of a one-dimensional gas with neighboring particles interacting by a repulsion potential. The theoretical results show a linear behavior of $\Delta_N(L)$ for large L —see (7). For completeness, we remark that numerical computations reveal that the approximations applied do not detract from the main analytical results (7)–(9), which are legitimate for all $\beta > 0$ and $L > 1$.

Using single-vehicle data measured on the Dutch freeway A9, the rigidity of the particle flow was evaluated. The statistical analysis of the data (based on the principle of data unfolding known from random matrix theory) shows a clear linear dependence of the rigidity of the traffic samples. The slope depends significantly on the traffic density. Also, the comparison of formula (7) with the traffic data has provided the possibility of detecting the mental strain of the car drivers moving in the traffic stream. The driver stress is indicated as the inverse temperature of the traffic sample. It shows an increase for low and high densities. In the intermediate region, where the free-flow regime converts to the congested traffic, it displays more complex behavior.

To conclude, we have shown that the microscopical structure of the traffic ensemble is rapidly changing with the traffic density and is well described by a one-parametric class of distributions (1) where the free parameter β is fixed by the traffic density ρ .

Acknowledgments

We are grateful to Dutch Ministry of Transport for providing the single-vehicle induction-loop-detector data. This work was supported by the Ministry of Education, Youth and Sports of the Czech Republic within the projects LC06002 and MSM 6840770039.

References

- [1] Kerner B S 2004 *The Physics of Traffic* (Berlin: Springer)
- [2] Helbing D 2001 *Rev. Mod. Phys.* **73** 1067
- [3] Knospe W, Santen L, Schadschneider A and Schreckenberg M 2004 *Phys. Rev. E* **70** 016115
- [4] Krbálek M 2008 *J. Phys. A: Math. Theor.* **41** 205004
- [5] Kerner B S, Klenov S L, Hiller A and Rehborn H 2006 *Phys. Rev. E* **73** 046107
- [6] Krbálek M and Helbing D 2004 *Physica A* **333** 370
- [7] Krbálek M 2007 *J. Phys. A: Math. Theor.* **40** 5813
- [8] Smith D, Marklof J and Wilson R E 2008 *Preprint* <http://hdl.handle.net/1983/1061>
- [9] Helbing D, Treiber M and Kesting A 2006 *Physica A* **363** 62
- [10] Helbing D and Treiber M 2003 *Phys. Rev. E* **68** 067101
- [11] Bogomolny E B, Gerland U and Schmit C 2001 *Eur. Phys. J. B* **19** 121
- [12] Mehta M L 2004 *Random Matrices* 3rd edn (New York: Academic Press)